Constructing Planar C^1 Cubic Hermite Interpolation Curves Via Approximate Energy Minimization

Juncheng LI

College of Mathematics and Finance, Hunan University of Humanities,
Science and Technology, Hunan 417000, P. R. China

Abstract The methods for constructing planar C^1 cubic Hermite interpolation curves via approximate energy minimization are studied. The main purpose of the proposed methods are to obtain the optimal tangent vectors of the C^1 cubic Hermite interpolation curves. By minimizing the appropriate approximate functions of the strain energy, the curvature variation energy and the combined energy, the linear equation systems for solving the optimal tangent vectors are obtained. It is found that there is no unique solution for the minimization of approximate curvature variation energy minimization, while there is unique solution for the minimization of approximate strain energy and the minimization of approximate combination energy because the coefficient matrix of the equation system is strictly diagonally dominant. Some examples are provided to illustrate the effectiveness of the proposed method in constructing planar C^1 cubic Hermite interpolation curves.

Keywords Hermite interpolation; strain energy; curvature variation; minimization

MR(2010) Subject Classification 65D07; 65D05

1. Introduction

It is known that the planar cubic Hermite interpolation curves can be described in the following Bézier form,

$$\mathbf{b}_i(t) = \mathbf{p}_i B_0^3(t) + (\mathbf{p}_i + \frac{1}{3}\mathbf{m}_i)B_1^3(t) + (\mathbf{p}_{i+1} - \frac{1}{3}\mathbf{m}_{i+1})B_2^3(t) + \mathbf{p}_{i+1}B_3^3(t), \qquad (1.1)$$

where $i = 0, 1, \ldots, n-1$, $\mathbf{p}_j \in \mathbb{R}^2$ $(j = 0, 1, \ldots, n)$ are distinct points, $\mathbf{m}_j \in \mathbb{R}^2$ $(j = 0, 1, \ldots, n)$ are tangent vectors, $B_k^3(t)$ $(k = 0, 1, 2, 3)$ are cubic Bernstein polynomials. It is clear that $\mathbf{b}_i(0) = \mathbf{p}_i$, $\mathbf{b}_i(1) = \mathbf{p}_{i+1}$, $\mathbf{b}'_i(0) = \mathbf{m}_i$, $\mathbf{b}'_i(1) = \mathbf{m}_{i+1}$, and $\mathbf{b}_i(t)$ satisfy C^1 continuity.

Generally, the C^1 Hermite interpolation curves problem requires that the tangent vectors are given in advance. But in practical applications the tangent vectors are rarely available. Since the tangent vectors have a significant influence on the shape of the curves, a natural question is how to choose them appropriately so that the curves satisfy preferable geometric features.

As we know, the fairness is an important geometric feature of a curve. The construction of fair curves is a fundamental issue in computer aided design (CAD) and related application

fields [1–3]. Although the fairness of a curve is difficult to be expressed in a quantitative way, the general ways to construct the fair curves are achieved by minimizing some energy functions [4]. In most cases, the strain energy (also called bending energy) minimization or the curvature variation energy minimization is adopted to achieve this goal [1,5–8].

Recently, a lot of works on constructing fair planar G^1 or G^2 Hermite interpolation curves via strain energy minimization or curvature variation energy minimization have been proposed [4,9–13]. Generally, the G^1 or G^2 continuity is called geometric continuity while C^1 or C^2 continuity is called parametric continuity. Although geometric continuity is a more appropriate geometric measurement of smoothness than parametric continuity, parametric continuity is still necessary in some applications [14]. Actually, the C^1 Hermite interpolation has been applied to many fields in recent years, such as modeling scientific data [15], reconstruction of the river beds [16], solving PDE [17], and so on. The motivation of this paper is to present the methods about how to choose the optimal tangent vectors by minimizing strain energy and curvature variation energy to obtain the fairest C^1 cubic Hermite interpolation curves. The rest of this paper is organized as follows. We give the method for constructing the tangent vectors by energy minimization in Section 2. Some examples are shown in Section 3. A short conclusion is given in Section 4.

2. Constructing tangent vectors via approximate energy minimization

The strain energy of the curve $\mathbf{b}_i(t)$ is defined by [1]

$$s_1(\mathbf{b}_i) = \int_0^1 [\kappa_i(t)]^2 \mathrm{d}t, \tag{2.1}$$

where $\kappa_i(t) = \frac{\|\mathbf{b}'_i(t) \times \mathbf{b}''_i(t)\|}{\|\mathbf{b}'_i(t)\|^3}$, $\mathbf{b}'_i(t)$ and $\mathbf{b}''_i(t)$ represents the first and the second derivative of $\mathbf{b}_i(t)$, respectively.

In order to simplify the calculation, the strain energy (2.1) is usually approximated by [10,18]

$$\hat{s}_1(\mathbf{b}_i) = \int_0^1 \|\mathbf{b}''_i(t)\|^2 \mathrm{d}t. \tag{2.2}$$

By a deduction from (1.1), we can obtain that

$$\mathbf{b}''_i(t) = 2(3\Delta\mathbf{p}_i - 2\mathbf{m}_i - \mathbf{m}_{i+1}) + 6(\mathbf{m}_i + \mathbf{m}_{i+1} - 2\Delta\mathbf{p}_i)t, \tag{2.3}$$

where $\Delta\mathbf{p}_i := \mathbf{p}_{i+1} - \mathbf{p}_i$.

From (2.3) the expression (2.2) becomes

$$\hat{s}_1(\mathbf{b}_i) = \int_0^1 \|2(3\Delta\mathbf{p}_i - 2\mathbf{m}_i - \mathbf{m}_{i+1}) + 6(\mathbf{m}_i + \mathbf{m}_{i+1} - 2\Delta\mathbf{p}_i)t\|^2 \mathrm{d}t$$

$$= 4(\|\mathbf{m}_i\|^2 + \|\mathbf{m}_{i+1}\|^2 + \mathbf{m}_i \cdot \mathbf{m}_{i+1} - 3\mathbf{m}_i \cdot \Delta\mathbf{p}_i - 3\mathbf{m}_{i+1} \cdot \Delta\mathbf{p}_i + 3\|\Delta\mathbf{p}_i\|^2). \tag{2.4}$$

From (2.4) the approximate strain energy of the whole C^1 curves can be expressed as

$$f_1(\mathbf{m}_0, \mathbf{m}_1, \ldots, \mathbf{m}_n) := \sum_{i=0}^{n-1} \hat{s}_1(\mathbf{b}_i)$$

$$=4\sum_{i=0}^{n-1}(\|\mathbf{m}_i\|^2 + \|\mathbf{m}_{i+1}\|^2 + \mathbf{m}_i\cdot\mathbf{m}_{i+1} - 3\mathbf{m}_i\cdot\Delta\mathbf{p}_i-$$
$$3\mathbf{m}_{i+1}\cdot\Delta\mathbf{p}_i + 3\|\Delta\mathbf{p}_i\|^2). \tag{2.5}$$

The curvature variation energy of the curve $\mathbf{b}_i(t)$ is defined by [19]

$$s_2(\mathbf{b}_i) = \int_0^1 [\kappa_i'(t)]^2 \mathrm{d}t. \tag{2.6}$$

According to (2.2), an approximate form of the curvature variation energy (2.6) can be approximately expressed as [12]

$$\hat{s}_2(\mathbf{b}_i) = \int_0^1 \|\mathbf{b}'''_i(t)\|^2 \mathrm{d}t. \tag{2.7}$$

By (2.3) we have

$$\mathbf{b}'''_i(t) = 6(\mathbf{m}_i + \mathbf{m}_{i+1} - 2\Delta\mathbf{p}_i). \tag{2.8}$$

From (2.8) the expression (2.7) becomes

$$\hat{s}_2(\mathbf{b}_i) = 36\int_0^1 \|\mathbf{m}_i + \mathbf{m}_{i+1} - 2\Delta\mathbf{p}_i\|^2 \mathrm{d}t$$
$$= 36(\|\mathbf{m}_i\|^2 + \|\mathbf{m}_{i+1}\|^2 + 2\mathbf{m}_i\cdot\mathbf{m}_{i+1} - 4\mathbf{m}_i\cdot\Delta\mathbf{p}_i - 4\mathbf{m}_{i+1}\cdot\Delta\mathbf{p}_i + 4\|\Delta\mathbf{p}_i\|^2). \tag{2.9}$$

From (2.9) the approximate curvature variation energy of the whole C^1 curves can be expressed as

$$f_2(\mathbf{m}_0, \mathbf{m}_1, \ldots, \mathbf{m}_n) := \sum_{i=0}^{n-1} \hat{s}_2(\mathbf{b}_i)$$
$$=36\sum_{i=0}^{n-1}(\|\mathbf{m}_i\|^2 + \|\mathbf{m}_{i+1}\|^2 + 2\mathbf{m}_i\cdot\mathbf{m}_{i+1} - 4\mathbf{m}_i\cdot\Delta\mathbf{p}_i-$$
$$4\mathbf{m}_{i+1}\cdot\Delta\mathbf{p}_i + 4\|\Delta\mathbf{p}_i\|^2). \tag{2.10}$$

Since the strain energy minimization and the curvature variation energy minimization are two general ways to construct the fair curves, one may obtain the optimal tangent vectors by minimizing $f_1(\mathbf{m}_0, \mathbf{m}_1, \ldots, \mathbf{m}_n)$ or $f_2(\mathbf{m}_0, \mathbf{m}_1, \ldots, \mathbf{m}_n)$. Alternatively, a natural idea also drives us to combine the strain energy minimization and the curvature variation energy minimization to obtain the optimal tangent vectors.

Here, we express the approximate combined energy of the curve $\mathbf{b}_i(t)$ as

$$\hat{s}_3(\mathbf{b}_i) = \hat{s}_1(\mathbf{b}_i) + \hat{s}_2(\mathbf{b}_i). \tag{2.11}$$

Then, from (2.4) and (2.9) the approximate combined energy of the whole C^1 curves can be expressed as

$$f_3(\mathbf{m}_0, \mathbf{m}_1, \ldots, \mathbf{m}_n) := \sum_{i=0}^{n-1} \hat{s}_3(\mathbf{b}_i) = \sum_{i=0}^{n-1} [\hat{s}_1(\mathbf{b}_i) + \hat{s}_2(\mathbf{b}_i)]$$

$$=4\sum_{i=0}^{n-1}(10\|\mathbf{m}_i\|^2 + 10\|\mathbf{m}_{i+1}\|^2 + 19\mathbf{m}_i \cdot \mathbf{m}_{i+1} - 39\mathbf{m}_i \cdot \Delta\mathbf{p}_i -$$
$$39\mathbf{m}_{i+1} \cdot \Delta\mathbf{p}_i + 39\|\Delta\mathbf{p}_i\|^2). \tag{2.12}$$

Denote $\frac{\partial f}{\partial \mathbf{m}_i} := (\frac{\partial f}{\partial m_i^x}, \frac{\partial f}{\partial m_i^y})^{\mathrm{T}}$, where $\frac{\partial f}{\partial m_i^x}$ and $\frac{\partial f}{\partial m_i^y}$ is the x-coordinate and the y-coordinate of $\mathbf{m}_i$, respectively. The following three cases are discussed.

Case 1 Approximate strain energy minimization.

The gradients of (2.5) can be calculated as follows,

$$\frac{\partial f_1}{\partial \mathbf{m}_0} = 4(2\mathbf{m}_0 + \mathbf{m}_1 - 3\Delta\mathbf{p}_0),$$

$$\frac{\partial f_1}{\partial \mathbf{m}_i} = 4[\mathbf{m}_{i-1} + 4\mathbf{m}_i + \mathbf{m}_{i+1} - 3(\Delta\mathbf{p}_{i-1} + \Delta\mathbf{p}_i)], \quad i = 1, 2, \ldots, n-1,$$

$$\frac{\partial f_1}{\partial \mathbf{m}_n} = 4(\mathbf{m}_{n-1} + 2\mathbf{m}_n - 3\Delta\mathbf{p}_{n-1}).$$

Then, by $\partial f_1/\partial \mathbf{m}_i = 0$, $i = 0, 1, \ldots, n$, we can obtain the following equation system of the approximate strain energy minimization,

$$\begin{cases} 2\mathbf{m}_0 + \mathbf{m}_1 = 3\Delta\mathbf{p}_0, \\ \mathbf{m}_{i-1} + 4\mathbf{m}_i + \mathbf{m}_{i+1} = 3(\Delta\mathbf{p}_{i-1} + \Delta\mathbf{p}_i), \quad i = 1, 2, \ldots, n-1, \\ \mathbf{m}_{n-1} + 2\mathbf{m}_n = 3\Delta\mathbf{p}_{n-1}. \end{cases} \tag{2.13}$$

We can see that system (2.13) is just the system of the natural cubic spline interpolation curves. Let $\mathbf{d}_0 = 3\Delta\mathbf{p}_0$, $\mathbf{d}_i = 3(\Delta\mathbf{p}_{i-1} + \Delta\mathbf{p}_i)$, $i = 1, 2, \ldots, n-1$, $\mathbf{d}_n = 3\Delta\mathbf{p}_{n-1}$, $\mathbf{d} = (\mathbf{d}_0, \mathbf{d}_1, \ldots, \mathbf{d}_n)^{\mathrm{T}}$, $\mathbf{m} = (\mathbf{m}_0, \mathbf{m}_1, \ldots, \mathbf{m}_n)^{\mathrm{T}}$, $A = (a_{i,j})$ be the coefficient matrix. Then the system (2.13) can be rewritten as

$$A\mathbf{m} = \mathbf{d}. \tag{2.14}$$

Let $k_i = \frac{1}{|a_{i,i}|}\sum_{j \neq i}|a_{i,j}|$. It is clear that $k := \max\{k_i\} = 1/2 < 1$, which shows the matrix A is strictly diagonally dominant. Therefore, system (2.14) has unique solution expressed by $\mathbf{m} = A^{-1}\mathbf{d}$. Then the function $f_1(\mathbf{m}_0, \mathbf{m}_1, \ldots, \mathbf{m}_n)$ has unique global minimum point at

$$\mathbf{m}_i = \sum_{j=0}^{n} c_{i,j}\mathbf{d}_j, \quad i = 0, 1, \ldots, n, \tag{2.15}$$

where $(c_{i,j}) := A^{-1}$.

Case 2 Approximate curvature variation energy minimization.

The gradients of (2.10) can be calculated as follows,

$$\frac{\partial f_2}{\partial \mathbf{m}_0} = 4(\mathbf{m}_0 + \mathbf{m}_1 - 2\Delta\mathbf{p}_0),$$

$$\frac{\partial f_2}{\partial \mathbf{m}_i} = 4[\mathbf{m}_{i-1} + 2\mathbf{m}_i + \mathbf{m}_{i+1} - 2(\Delta\mathbf{p}_{i-1} + \Delta\mathbf{p}_i)], \quad i = 1, 2, \ldots, n-1,$$

$$\frac{\partial f_2}{\partial \mathbf{m}_n} = 4(\mathbf{m}_{n-1} + \mathbf{m}_n - 2\Delta\mathbf{p}_{n-1}).$$

Then, by $\partial f_2/\partial \mathbf{m}_i = 0$, $i = 0, 1, \ldots, n$, we can obtain the following equation system of the approximate curvature variation energy minimization,

$$\begin{cases} \mathbf{m}_0 + \mathbf{m}_1 = 2\Delta\mathbf{p}_0, \\ \mathbf{m}_{i-1} + 2\mathbf{m}_i + \mathbf{m}_{i+1} = 2(\Delta\mathbf{p}_{i-1} + \Delta\mathbf{p}_i), \quad i = 1, 2, \ldots, n-1, \\ \mathbf{m}_{n-1} + \mathbf{m}_n = 2\Delta\mathbf{p}_{n-1}. \end{cases} \tag{2.16}$$

It is not difficult to verify that the coefficient matrix of system (2.16) is singular. That is to say, there is no unique solution for the system (2.16).

Case 3 Approximate combined energy minimization.

The gradients of (2.12) can be calculated as follows,

$$\frac{\partial f_3}{\partial \mathbf{m}_0} = 4(20\mathbf{m}_0 + 19\mathbf{m}_1 - 39\Delta\mathbf{p}_0),$$

$$\frac{\partial f_3}{\partial \mathbf{m}_i} = 4[19\mathbf{m}_{i-1} + 40\mathbf{m}_i + 19\mathbf{m}_{i+1} - 39(\Delta\mathbf{p}_{i-1} + \Delta\mathbf{p}_i)], \quad i = 1, 2, \ldots, n-1,$$

$$\frac{\partial f_3}{\partial \mathbf{m}_n} = 4(19\mathbf{m}_{n-1} + 20\mathbf{m}_n - 39\Delta\mathbf{p}_{n-1}).$$

Then, by $\partial f_3/\partial \mathbf{m}_i = 0$, $i = 0, 1, \ldots, n$, we can obtain the following equation system of the approximate combined energy minimization,

$$\begin{cases} 20\mathbf{m}_0 + 19\mathbf{m}_1 = 39\Delta\mathbf{p}_0, \\ 19\mathbf{m}_{i-1} + 40\mathbf{m}_i + 19\mathbf{m}_{i+1} = 39(\Delta\mathbf{p}_{i-1} + \Delta\mathbf{p}_i), \quad i = 1, 2, \ldots, n-1, \\ 19\mathbf{m}_{n-1} + 20\mathbf{m}_n = 39\Delta\mathbf{p}_{n-1}. \end{cases} \tag{2.17}$$

Let $B = (b_{i,j})$ be the coefficient matrix. Then the system (2.17) can be rewritten as

$$B\mathbf{m} = 13\mathbf{d}. \tag{2.18}$$

Let $l_i = \frac{1}{|b_{i,i}|}\sum_{j\neq i}|b_{i,j}|$. It is clear that $l := \max\{l_i\} = \frac{19}{20} < 1$, which shows the matrix B is strictly diagonally dominant. Thus system (2.18) has unique solution expressed by $\mathbf{m} = 13B^{-1}\mathbf{d}$. Then the function $f_3(\mathbf{m}_0, \mathbf{m}_1, \ldots, \mathbf{m}_n)$ has unique global minimum point at

$$\mathbf{m}_i = 13\sum_{j=0}^{n} h_{i,j}\mathbf{d}_j, \quad i = 0, 1, \ldots, n, \tag{2.19}$$

where $(h_{i,j}) := B^{-1}$.

Notice that the systems (2.13) and (2.17) contain the equations about the x-coordinate and the y-coordinate. Due to the fact that the coefficient matrixes are tri-diagonal, the solutions of system (2.13) and (2.17) can be obtained easily by the LU factorization method.

At the end of this section, we give the method for constructing closed curves. In order to obtain closed curves, we set $\mathbf{p}_n = \mathbf{p}_0$ and $\mathbf{m}_n = \mathbf{m}_0$. Then, by $\partial f_1/\partial \mathbf{m}_0 = 0$, corresponding to the first equation and the last equation of (2.13), we have $4\mathbf{m}_0 + \mathbf{m}_1 + \mathbf{m}_{n-1} = 3(\mathbf{p}_1 - \mathbf{p}_{n-1})$. We can discuss the equation $\partial f_1/\partial \mathbf{m}_{n-1} = 0$ in the same way, and then we have $\mathbf{m}_0 + \mathbf{m}_{n-2} + 4\mathbf{m}_{n-1} = 3(\mathbf{p}_0 - \mathbf{p}_{n-2})$.

For $i = 1, 2, \ldots, n-2$, we can obtain the same system as (2.13) in form. Hence, for the closed curves, the system of the approximate strain energy minimization can be expressed as

$$\begin{cases} 4\mathbf{m}_0 + \mathbf{m}_1 + \mathbf{m}_{n-1} = 3(\mathbf{p}_1 - \mathbf{p}_{n-1}), \\ \mathbf{m}_{i-1} + 4\mathbf{m}_i + \mathbf{m}_{i+1} = 3(\mathbf{p}_{i+1} - \mathbf{p}_{i-1}), \quad i = 1, 2, \ldots, n-2, \\ \mathbf{m}_0 + \mathbf{m}_{n-2} + 4\mathbf{m}_{n-1} = 3(\mathbf{p}_0 - \mathbf{p}_{n-2}). \end{cases} \tag{2.20}$$

Similarly, for closed curves, the system of the approximate combined energy minimization can be expressed as

$$\begin{cases} 40\mathbf{m}_0 + 19\mathbf{m}_1 + 19\mathbf{m}_{n-1} = 39(\mathbf{p}_1 - \mathbf{p}_{n-1}), \\ 19\mathbf{m}_{i-1} + 40\mathbf{m}_i + 19\mathbf{m}_{i+1} = 39(\mathbf{p}_{i+1} - \mathbf{p}_{i-1}), \quad i = 1, 2, \ldots, n-2, \\ 19\mathbf{m}_0 + 19\mathbf{m}_{n-2} + 40\mathbf{m}_{n-1} = 39(\mathbf{p}_0 - \mathbf{p}_{n-2}). \end{cases} \tag{2.21}$$

3. Numerical examples

We present some examples generated by the approximate strain energy minimization (viz. the natural cubic spline interpolation curves) and the approximate combined energy minimization in this section.

We first illustrate the effects of the presented method by taking the points as $\mathbf{p}_0 = (1, 90)$, $\mathbf{p}_1 = (3, 105)$, $\mathbf{p}_2 = (6, 120)$, $\mathbf{p}_3 = (10, 100)$, $\mathbf{p}_4 = (12, 85)$, $\mathbf{p}_5 = (15, 104)$, $\mathbf{p}_6 = (17, 80)$. Figure 1 shows the interpolation curves.

The second example is to consider the monotone points set for $\mathbf{p}_0 = (-3, -3)$, $\mathbf{p}_1 = (-1, -2)$, $\mathbf{p}_2 = (0, 0)$, $\mathbf{p}_3 = (3, 1)$, $\mathbf{p}_4 = (5, 2)$, $\mathbf{p}_5 = (6, 4)$. Figure 2 shows the interpolation curves.

The third example is to consider different number of points sampled from a unit semicircle $\mathbf{r}(t) = (\cos(\pi t), \sin(\pi t))^{\mathrm{T}}$, $t \in [0, 1]$. Figure 3 shows the interpolation curves.

The fourth example is to consider the points taken from function $f(x) = x \sin x$, $x = 0 : 1 : 8$. Figure 4 shows the interpolation curves.

The last example is to consider the case of closed curves. The points are taken from an ellipse $\mathbf{r}(t) = (2\cos(2\pi t), \sin(2\pi t))^{\mathrm{T}}$, $t \in [0, 1]$. Figure 5 shows the interpolation curves.
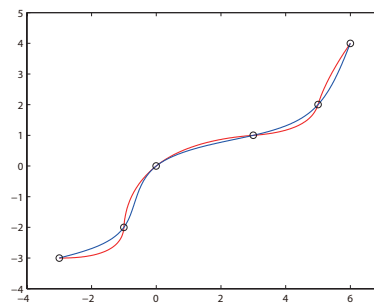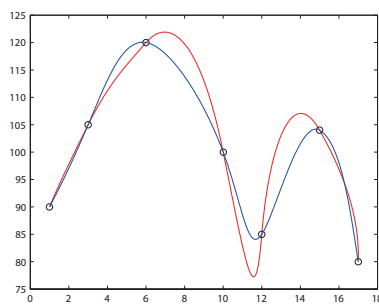

Figure 1 Interpolating the given data   Figure 2 Interpolation of the monotone points

In Figures 1–5, the red lines represent the curves obtained by minimizing the approximate combined energy, the blue lines represent the natural cubic spline interpolation curves, and the

circle points represent the given points, respectively. For Figures 3–5, the dashed lines represent the sampled curves.

(a) 3 sampling points

(b) 5 sampling points

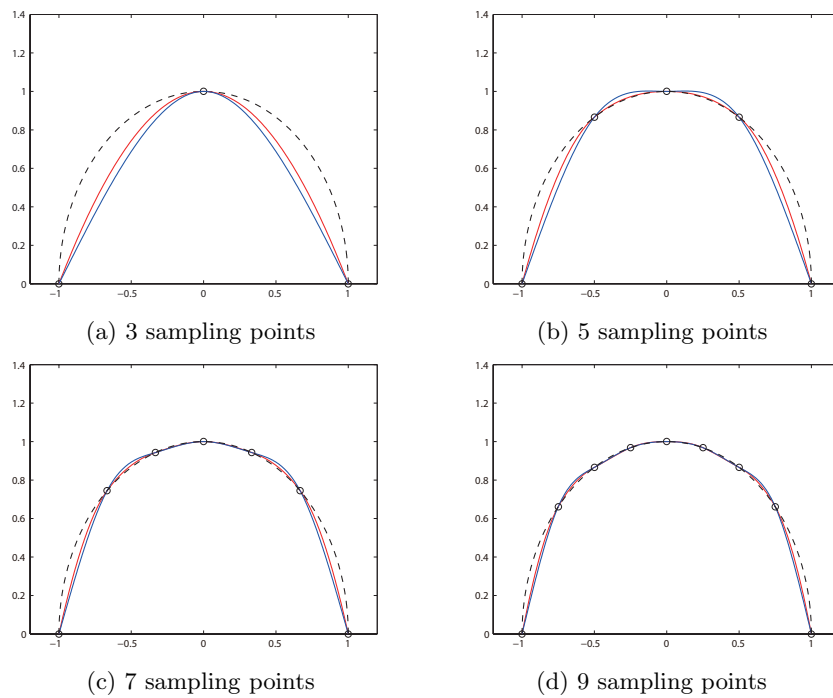(c) 7 sampling points

(d) 9 sampling points

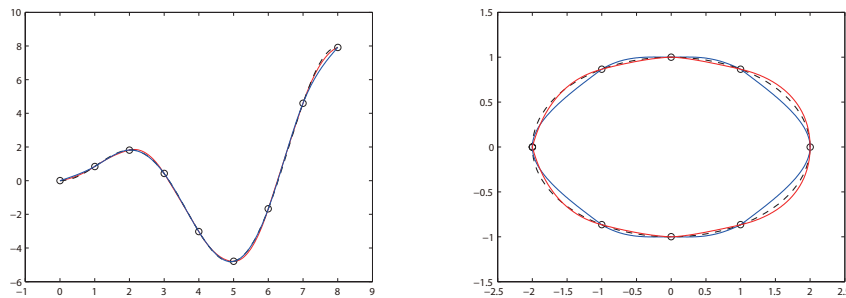Figure 3 Interpolating a unit semicircle

Figure 4 Interpolating the function $x \sin x$ Figure 5 Interpolating an ellipse

The above examples show that both the natural cubic spline interpolation curves and the curves obtained by the combined energy minimization can achieve good interpolation results. Furthermore, Figure 3 shows that the approximation effect becomes better as the number of the sampling points becomes larger and the curves by minimizing the approximate combined energy give a better approximation than the natural cubic spline interpolation curves; Figures 3–5 show that the curves obtained by the approximate combined energy minimization give a more pleasant approximation than the natural cubic spline interpolation curves.

4. Conclusions

This paper discusses the methods for constructing the fair cubic C^1 Hermite interpolation curves by minimizing the approximate energy functions. Our method focuses on how to construct the optimal tangent vectors, which is achieved by minimizing the appropriate approximate functions of the strain energy, curvature variation energy and combined energy. Results show that the approximate curvature variation energy minimization has no unique solution, and approximate combined energy minimization provides a more satisfactory approximation than the approximate strain energy minimization.

References

[1] G. FARIN. *Curves and surfaces for CAGD: A Practical Guide*. Academic Press, San Diego, 2002.

[2] M. HOFER, H. POTTMANN. *Energy-minimizing splines in manifolds*. ACM T. Graphic., 2004, **23**(3): 284–93.

[3] Wei FAN, C. H. LEE, Jihong CHEN. *A realtime curvature-smooth interpolation scheme and motion planning for CNC machining of short line segments*. Int. J. Mach. Tool Manu., 2015, **96**: 27–46.

[4] Lizheng LU, Chengkai JIANG, Qianqian HU. *Planar cubic G^1 and quintic G^2 Hermite interpolations via curvature variation minimization*. Comput. Graph., 2017, **70**: 92–98.

[5] G. FARIN. *Geometric Hermite interpolation with circular precision*. Comput. Aided Geom. Design, 2008, **40**(4): 476–479.

[6] R. J. RENKA. *Shape-preserving interpolation by fair discrete G^3 space curves*. Comput. Aided Geom. Design, 2005, **22**(8): 793–809.

[7] Gang XU, Guozhao WANG, Wenyu CHEN. *Geometric construction of energy-minimizing Bézier curves*. Sci. China Inform. Sci., 2011, **54**(7): 1395–1406.

[8] Y. J. AHN, C. HOFFMANN, P. ROSEN. *Geometric constraints on quadratic Bézier curves using minimal length and energy*. J. Comput. Appl. Math., 2014, **255**: 887–897.

[9] Junhai YONG, Fuhua CHENG. *Geometric Hermite curves with minimum strain energy*. Comput. Aided Geom. Design, 2004, **21**(3): 281–301.

[10] G. JAKLIČ, E. ŽAGAR. *Planar cubic G1 interpolatory splines with small strain energy*. J. Comput. Appl. Math., 2011, **235**(8): 2758–2765.

[11] G. JAKLIČ, E. ŽAGAR. *Curvature variation minimizing cubic Hermite interpolants*. Appl. Math. Comput., 2011, **218**(7): 3918–3924.

[12] Lizheng LU. *A note on curvature variation minimizing cubic Hermite interpolants*. Appl. Math. Comput., 2015, **259**: 596–599.

[13] Lizheng LU. *Planar quintic G^2 Hermite interpolation with minimum strain energy*. J. Comput. Appl. Math., 2015, **274**: 109–117.

[14] C. L. TAI, K. F. LOE. *Alpha-spline: A C^2 continuous spline with weights and tension control*. Proceedings of the International Conference on Shape Modeling and Applications, Mar. 1999, Aizu-Wakamatsu, Japan.

[15] R. J. CRIPPS, M. Z. HUSSAIN. *C^1 monotone cubic Hermite interpolant*. Appl. Math. Lett., 2012, **25**(8): 1161–1165.

[16] C. V. DANIEL, M. H. MARIO, L. M. IBAI, et al. *Reconstruction of 2D river beds by appropriate interpolation of 1D cross-sectional information for flood simulation*. Environ. Modell. Software, 2014, **61**(C): 206–228.

[17] T. HAGSTROM, D. APPELÖ. *Solving PDEs with Hermite Interpolation*. Springer, Cham, 2015.

[18] J. WALLNER. *Note on curve and surface energies*. Comput. Aided Geom. Design, 2007, **24**(8-9): 494–498.

[19] G. FARIN. *Geometric Hermite interpolation with circular precision*. Comput. Aided Geom. Design, 2008, **40**(4): 476–479.